INTERNATIONAL JOURNAL OF PARALLEL, EMERGENT AND DISTRIBUTED SYSTEMS, 2017
VOL. 32, NO. 3, 295–305
http://doi.org/10.1080/17445760.2017.1316908

Taylor & Francis
Taylor & Francis Group

Noise assisted image processing by ensembles of R-SETs

J. Cervera, J. A. Manzanares and S. Mafe

School of Physics, University of Valencia, Burjassot, Spain

ABSTRACT

We study how noise can assist the processing of an image in a resistance-single electron transistor (R-SET) model. The image is an 8-bit black and white picture. Every grey level is codified linearly into a sub-threshold input potential applied for a prescribed time window to an ensemble of R-SETs that transforms it into a spiking frequency. The addition of a background white noise potential of high amplitude permits the ensemble to process the image by means of the stochastic resonance phenomenon. Aside from the positive aspects, we analyse the negative impact of using noise and how we can minimize it using redundancy and a longer measuring time. The results are compared with the case of the addition of a constant potential to the codified potential to scale it up to the supra-threshold regime.

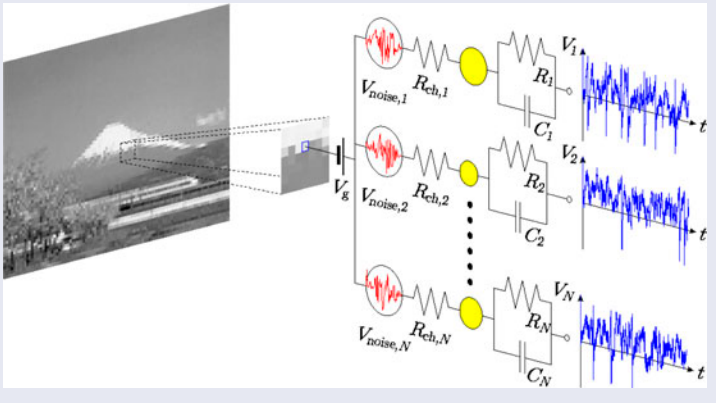

A background white noise potential of high amplitude permits an ensemble of R-SET units to process an image by means of the stochastic resonance phenomenon. The negative impacts can be minimized using redundancy and a longer measuring time.

ARTICLE HISTORY
Received 11 November 2015
Accepted 20 December 2015

KEYWORDS
Resistance-single electron transistor (R-SET); image processing; noise assisted detection; stochastic resonance; redundancy

1. Introduction

The importance of noise unrelently grows as the size of the basic unit of an electronic device shrinks [1–6]. Noise can be static, such as the component diversity inherent to the nanoscale, and dynamic, such as thermal noise. Together with weak signals, quite common when we deal with nanostructures, noise can easily render our signal processing device useless. If we want a fully operational device based on nanoelectronics, we need to tackle the noise problem.

Nature has managed to achieve a robust information processing using nanoscale basic units despite operating in a noisy environment [7–12]. Two concepts, stochastic resonance and redundancy, are

CONTACT J. Cervera javier.cervera@uv.es

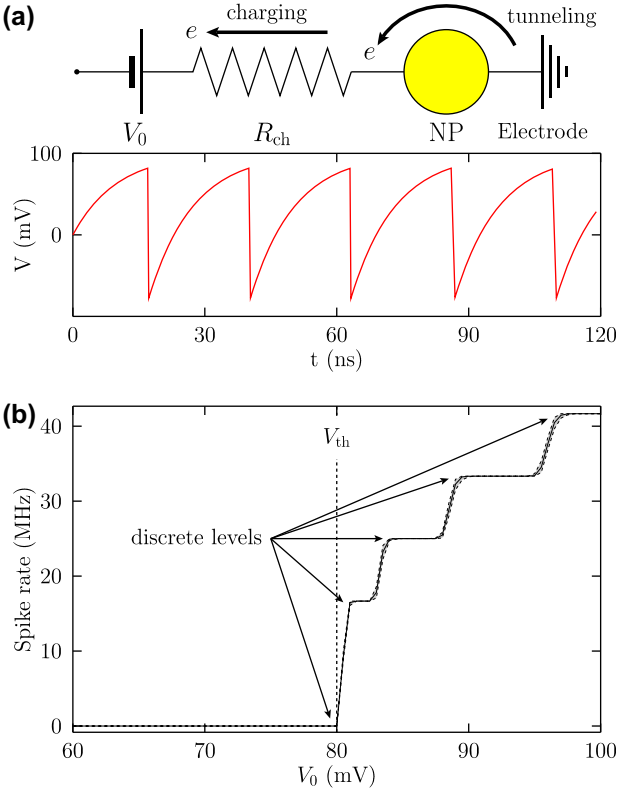

Figure 1. (a) Scheme of the R-SET model. When a potential $V_0 > V_{th}$ is applied, a charging-tunnelling process occurs that generates periodic oscillations of the NP potential V. The parameters are $R_{ch} = 10$ GΩ and $C = 1$ aF. Temperature is 5 K. (b) Transduction of a signal (V_0) into discrete spiking (tunnelling events) frequencies by an ensemble of 100 R-SETs using a time window of 120 ns.

considered to be used by the brain to assist reliable processing [7,8,13–17]. If we can master stochastic resonance, noise can be used to our own benefit [18–20]. This benefit would be further improved when redundancy is combined with stochastic redundancy [18].

In this work we analyse how noise can assist the image processing of weak signals, similarly to the benefitial effects observed in the detection of visual, hearing, and tactile weak stimulus in humans [16]. We use the R-SET system [21–23], a simple integrate-and-fire model which mimics some aspects of the neurons behaviour [24,25]. The addition of white noise allows the detection of a weak signal. However, the detected signal shows fluctuations that need to be partially cancelled to achieve the given prescribed signal-to-noise ratio needed for image processing. This can be accomplished by the use of redundancy [7,13] when noise is white and the units share the same signal but their associated noise is independent. If noise is common to all the units in the array, we can achieve similar results by integrating in time [13].

2. Related work

The R-SET model (Figure 1(a)) [21–23] consists of a (molecularly protected) metallic nanoparticle (NP) linked to an electrode (ground potential) by a ligand that acts as a tunnelling junction [24,25]. The NP then behaves like a single electron transistor (SET) and its equivalent circuit is formed by a capacitance C in parallel to a tunnelling junction of resistance R. A 'charging' resistance R_{ch} connects the SET to another electrode at potential V_0. Because the capacitance associated with the NP is of the order of 1 aF (10^{-18} F), there is an energy penalty to add an electron to or remove it from the NP. This phenomenon is known as Coulomb blockade [3,20,27]. When a constant supra-threshold potential V_0 is applied to

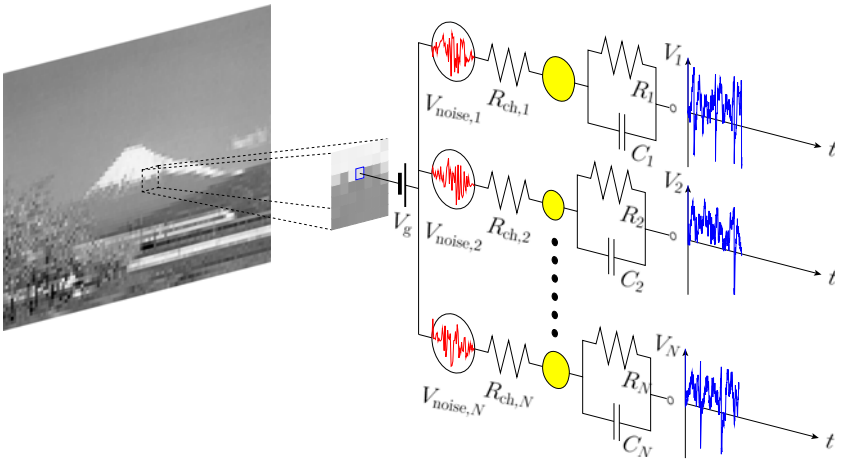

Figure 2. Image processing using an ensemble of R-SETs. The pixel grey level is codified into a potential. This potential is in the sub-threshold range but can be detected with the help of a white noise potential.

the NP through the charging resistance, the NP potential slowly increases (charging process). When the NP potential V reaches the threshold value $V_{\text{th}} = e/2C$, where e is the elementary charge, an electron tunnels from the electrode to the NP and lowers the NP potential a value $-2V_{\text{th}}$ (tunnelling). The charging of the NP resumes until the next tunnelling event, giving the charging-tunnelling oscillations of Figure 1(a). This sequence can be disrupted when the thermal energy kT, where k is the Boltzmann constant and T is the temperature, is of the order or higher than the energy penalty eV_{th}. In Figure 1 the temperature used in the calculation was 5 K to assure that $kT \ll eV_{\text{th}}$. In addition, the charging resistance needs to be much higher than the tunnelling resistance so that the charging process takes much longer than the tunnelling process.

In a previous work we analysed how the R-SET model could provide some insights on the processing of images made by the neurons [24,25]. The grey tone of an image was transformed into an input potential V_0 that was applied to an ensemble of R-SET units arranged in parallel. The R-SETs transducted the input potential into a series of spikes (tunnelling events) whose frequency depended on V_0. Because the response of the ensemble was between $V_0 = 60$ mV and $V_0 = 100$ mV [25], if an image was codified to potentials lower than the detection limit of 60 mV it became undetectable. This also happens in other threshold systems, like the human vision. In this case, it has been shown that adding external noise to a visual weak signal below the detection limit allows for its detection [26]. Following this example, we analyse in this work if a sub-threshold signal can be detected by an ensemble of R-SETs assisted by the addition of a white noise.

3. Procedure

We study the image processing of an ensemble of R-SETs units (Figure 2). The input image is codified into a potential that is applied to every R-SET in the ensemble. Because the potential used is sub-threshold, we scale it up to the supra-threshold region by adding either a constant offset potential or a white noise. The average frequency of the tunnelling events (spikes) of the ensemble is used as the output magnitude of the processed image.

3.1. The charging-tunnelling process

Every R-SET i in the ensemble (Figure 1) is composed of a NP linked to an electrode (ground potential) by a ligand acting as a tunnelling junction. The ligand-protected NP behaves as a SET and its equivalent circuit consists of a capacitance C_i in parallel to a tunnelling junction of resistance R_i. A 'charging' resistance $R_{\text{ch},i}$ connects the SET to another electrode at potential V_0.

At low temperatures, the Coulomb blockade gives the charging-tunnelling oscillations of Figure 1(a). The time variation of the potential V_i of the NP due to the charging process can be described by the equation

$$\frac{dV_i}{dt} = \frac{V_{0,i} - V_i}{R_{ch,i}C_i} \tag{1}$$

and depends on the characteristic time $R_{ch,i}C_i$ and the applied potential $V_{0,i}$. Tunnelling can be described as a stochastic process of rate [24,25]

$$\Gamma_i = \frac{1}{e^2 R_i} \frac{-\Delta E_i}{1 - \exp(\Delta E_i / kT)} \tag{2}$$

when the tunnelling junction resistance R_i is much higher than the quantum resistance $R_h = h/2e$, where h is the Planck constant. In Equation (2), k is the Boltzmann constant and

$$\Delta E_i = e(V_i - V_{i,th}) \tag{3}$$

is the change in electrostatic energy due to the electron tunnelling.

The charging-tunnelling oscillations of the R-SET are calculated by integrating numerically Equation (1), checking the possibility of a tunnelling event at every time step. We first set the initial value of the NP potential $V_i(t = 0) = 0$. The applied potential to the R-SET is

$$V_{0,i}(t) = V_g + \begin{cases} V_{off} \\ V_{noise,i}(t) \end{cases} \tag{4}$$

because V_g is scaled up by the addition of a constant offset potential V_{off} or a white noise. When the white noise potential $V_{noise,i}(t)$ of amplitude $V_{noise,max}$ is added to V_g, a random value between $-V_{noise,max}$ and $V_{noise,max}$ mV is calculated from an uniform distribution every $\Delta t_{noise} = 1$ ns. At every time step $\Delta t = 10$ ps of the charging equation, the NP potential is updated

$$V_i(t + \Delta t) = V_i(t) + \frac{V_{0,i}(t) - V_i(t)}{R_{ch,i}C_i} \Delta t \tag{5}$$

Then, the rate of a tunnelling process either from the electrode to the NP or from the NP to the electrode is calculated using Equation (2) (for the 'backwards' tunnelling event, the energy is $-e(V_i + V_{th,i})$). A transition 'rate' $\Gamma_{ch} = 1/\Delta t$ is assigned to the charging process. Then a kinetic Monte Carlo algorithm is used to check which one of the three options (charging, electrode→NP tunnelling, NP→electrode tunnelling) comes at the next step. If a tunnelling event occurs the NP is decreased (electrode→NP) or increased (NP→electrode) by an amount $2V_{th,i}$. The calculation continues until the simulating time reaches the prescribed time for every R-SET. Finally, the net number of tunnelling events (net charge transferred for the electrode to the NP) is summed for every R-SET and divided by the prescribed time to obtain the spiking frequency.

3.2. Image processing

The original image is an 8-bit black and white image, where every pixel has a grey level between $g = 0$ (black) and $g = 255$ (white). The grey level is then transformed linearly into an input potential between $V_{g,min} = 0$ (black) and $V_{g,max}$ (white)

$$V_g = V_{g,max} \frac{g}{255} \ (0 \le g \le 255) \tag{6}$$

Because we consider $V_{g,max} < V_{th}$, no spiking event would be obtained if V_g was applied directly to the ensemble of R-SETs. To process the image we scale up V_g to the supra-threshold regime. This is

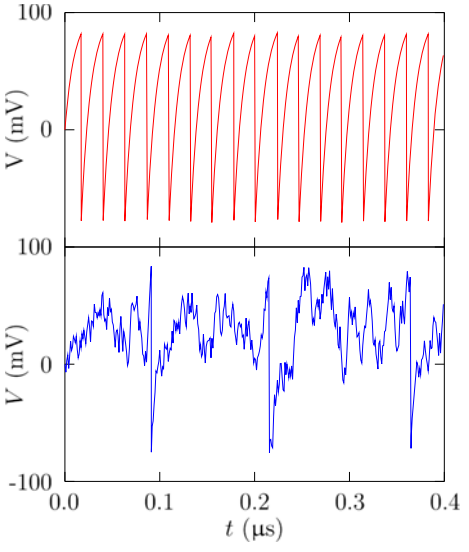

Figure 3. NP potential for a R-SET for $V_0 = 100$ mV (top) or $V_0 = 40$ mV $+ V_{\text{noise}}$, where V_{noise} is a white noise of peak-to-peak amplitude 200 mV and a characteristic time of 1 ns (bottom).

first done by adding a constant offset potential V_{off} to the codified potential of Equation (6) so that the input potential $V_0 = V_{\text{g}} + V_{\text{off}} > V_{\text{th}}$ is in the supra-threshold regime. The second option to scale up the sub-threshold input signal is the addition of a white noise.

The input potential is applied for a prescribed time window to an ensemble of R-SETs that transforms it into a spiking frequency, where every spike is a tunnelling event (see Figure 1). The average spiking frequency is calculated as the total number of spikes divided by the number of R-SETs in the ensemble and the measuring time. To show the result of the image processing, the average spiking frequency of every pixel $\overline{\nu}$ is converted to a grey level g_{p} to reconstruct the image. Black is assigned to zero frequency (no spikes) and white is assigned a prescribed frequency $\overline{\nu}_{\text{white}}$ related to the highest average frequency that can be obtained for $V_{\text{g,max}}$ in the detection window time (see Figure 5 below)

$$g_{\text{p}} = \frac{\overline{\nu}}{\overline{\nu}_{\text{white}}} \tag{7}$$

4. Results

Unless otherwise stated, every R-SET is characterised by the charging resistance $R_{\text{ch}} = 10$ GΩ, the tunnelling resistance $R_{\text{tun}} = 10$ MΩ and the capacitance $C = 1$ aF, which gives a threshold potential $V_{\text{th}} = e/2C \approx 80$ mV [24,25]. The temperature of the R-SETs is $T = 5$ K. An offset potential $V_{\text{off}} = 60$ mV or a white noise of amplitude $V_{\text{noise,max}} = 200$ mV and characteristic time 1 ns is used to scale up the sub-threshold potential V_{g}. This characteristic time can be compared with $R_{\text{ch}}C = 10$ ns, which gives the order of magnitude of the charging process in the absence of noise.

4.1. Charging-tunnelling

Figure 3 shows the charging-tunnelling processes in an R-SET system in the absence and presence of the background white noise. In the absence of noise, the applied voltage is $V_0 = 100$ mV $> V_{\text{th}}$. Because the applied voltage is higher than the threshold voltage and the temperature is sufficiently low, we can see the charging-tunnelling oscillations. In the presence of noise $V_0 = 40$ mV $+ V_{\text{noise}}(t)$, Figure 3 shows that the charging process now needs a longer time to be completed. Also, the charging time may differ significantly between tunnelling events, showing a wide distribution (Figure 4).

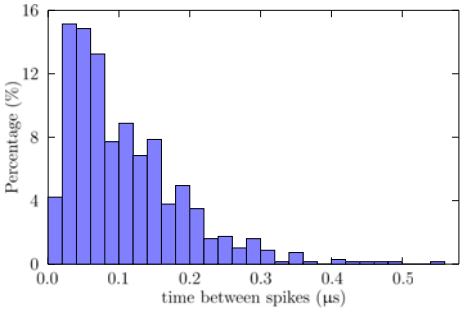

Figure 4. Distribution of time between spikes for a single R-SET under a potential $V_0 = 40$ mV $+ V_{\text{noise}}$, where V_{noise} is a white noise of amplitude 200 mV and a characteristic time of 1 ns.

To process an image using the R-SET ensemble, we need first to define a measuring time window and analyse the spiking rate as a function of the applied voltage. We consider the case where the input potential V_g, that will codify the image, is in the range $0 \leq V_g \leq 40$ mV, well below the threshold potential. The potential V_g is scaled it up toward the supra-threshold regime either by the addition of an offset potential V_{off} (the potential applied is then $V_0 = V_g + V_{\text{off}}$ and lies between 60 mV and 100 mV (see Figure 1(b)) or by adding a different white noise $V_{\text{noise},i}(t)$ to every R-SET i (in this case the applied potential $V_{0,i} = V_g + V_{\text{noise},i}(t)$).

Figure 5 shows the average spiking rate, estimated as the total number of tunnelling events of the ensemble per R-SET per unit time, for an ensemble of 100 identical R-SETs and a time window of 150 ns. Figure 5(a) shows the case were a constant offset potential has been added to V_g. There are no spiking events for $V_g < 20$ mV, which corresponds to $V_0 < V_{\text{th}}$. Because the charging time depends on V_0, when $V_0 > V_{\text{th}}$, the number of spiking (tunnelling) increases with V_0. For $V_g = 40$ mV ($V_0 = 100$ mV) there are 5 spiking events in the time window. The input potential V_g is transformed into a discrete number of average spiking frequencies (output). Figure 5(b) shows the case where white noise is added to the input potential V_g. In this case the charging time is no longer constant (see Figure 3) but has a wide distribution (see Figure 4). To obtain meaningful results, the simulation was repeated 100 times for every applied voltage V_g. The central line is the average value obtained from the total number of simulations whereas the grey regions are defined between the highest and the lowest frequencies obtained. This is done in Figure 5(a) as well. However, in this case only the thermal noise (very low at 5 K) gives the differences among the simulations. In Figure 5(b) we observe how the average rate increases *gradually* with V_g due to the addition of white noise.

A perfect image processing would need a one-to-one correspondence between the input potential and the output frequency. This is not achieved here. When a constant offset potential was added to V_g the limited time window reduces the 256 initial levels to 6. By contrast, when white noise is added, the fluctuations associated with the noise create a zone of uncertainty around the average value. Although this uncertainty is reduced because the noise is white and local to every R-SET and an ensemble is used (redundancy), it is not completely eliminated. Despite these problems, a one-to-one relationship can be roughly defined in both cases. Better results could be obtained at the expense of a longer measuring time (in both cases) or of a larger ensemble (in the white noise case).

4.2. Image processing

Figure 6 shows the processing of an image by an ensemble of 100 identical R-SETs. The grey levels of the original image are transformed linearly into an input potential between $V_{g,\text{min}} = 0$ (black) and $V_{g,\text{max}} = 40$ mV (white). In the reconstruction of the image after being processed by the ensemble, black is assigned to zero frequency (no spikes) and white is assigned to an average frequency $\overline{\nu}_{\text{white}} = 40$ MHz, when an offset potential V_{off} is employed, or $\overline{\nu}_{\text{white}} = 10$ MHz, when a white noise potential is employed (see Figure 5(a)).

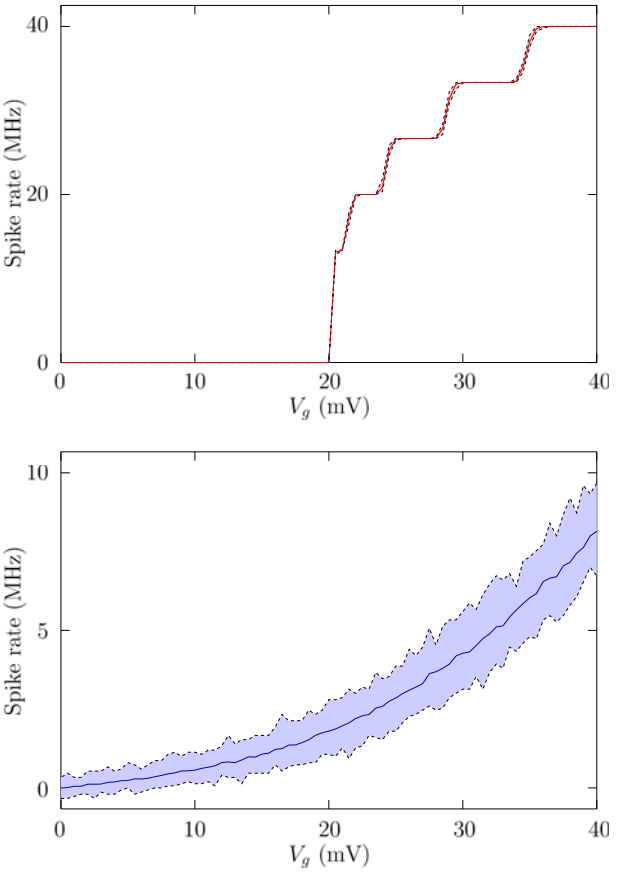

Figure 5. Average spiking rate (number of spiking events per unit time) for an ensemble of 100 identical R-SETs when the applied voltage is $V_0 = V_g + V_{off}$, $V_{off} = 60$ mV, (a) or $V_0 = V_g + V_{noise}$, where V_{noise} is a white noise of amplitude 200 mV and characteristic time 1 ns (b). The time window is 150 ns.

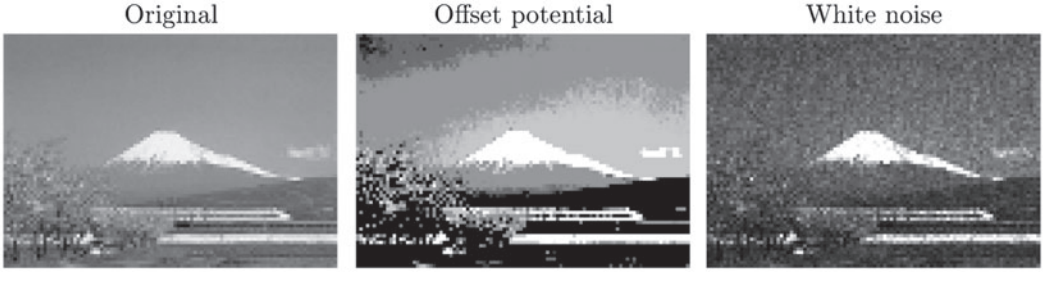

Figure 6. Image processing by an ensemble of 100 R-SETs using a sub-threshold input potential scaled up to the supra-threshold regime by the addition of an offset potential or a white noise.

Figure 6 shows that either adding a constant offset potential or adding white noise allows to process the image. In the first case, the image is reduced from 256 grey levels to 6. Some saturation (a shift to white in regions of the image) is also shown. In the second case, the processed image shows some noise that could not be cancelled out.

We could think how the image processing could be improved. In the case of the added offset potential, the number of allowed frequencies increases (and then the levels of grey) when the time

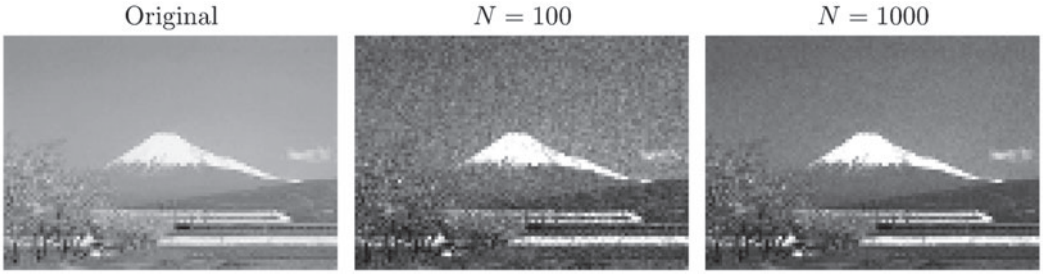

Figure 7. Image processing by an ensemble of 100 R-SETs or 1000 R-SETs using a sub-threshold input potential scaled up to the supra-threshold regime by the addition of a white noise.

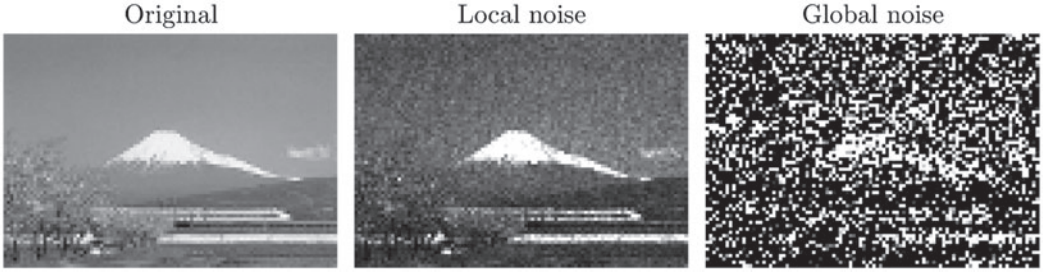

Figure 8. Image processing by an ensemble of 100 R-SETs using a sub-threshold input potential scaled up to the supra-threshold regime by the addition of a white noise that is either different (local) or the same (global) for every R-SET of the ensemble.

window is increased. This results in an improved image processing. In the case of the addition of white noise, we could improve the image processing by increasing the number of R-SETs in the ensemble. This is shown in Figure 7, where this number is increased tenfold up to 1000 R-SETs. The improvement in the image processing is clear. However, it should be considered whether the benefit of an improved processing is worth the increase of the number of R-SETs (and then the increase in size).

4.2.1. Local noise vs global noise

The addition of noise allows for the processing of the image in Figures 6 and 7. However, image processing not only implies the detection of the signal, but also the correspondence between the original image and the processed image. Because the noise in Figures 6 and 7 is white and local to every R-SET in the ensemble, the sum of the responses of the R-SETs can harness the benefits of the noise (the detection of a sub-threshold signal) while minimising the fluctuations that are partially cancelled out.

The situation is very different when the noise is not local but global, that is, when we have the same noise for every R-SET in the ensemble. The comparison of local noise (different for every R-SET in the ensemble) and global noise (the same for every R-SET in the ensemble) is shown in Figure 8. In the latter case the fluctuations cannot be cancelled out, as all R-SET 'see' the same noise (noise helps in detecting a signal but not in processing the image).

To improve the image processing when the noise is global we consider first the use of an ensemble of non-identical R-SETs because heterogeneous units may bring the benefits of a different individual response [7,24,25,28,29]. A different charging resistance $R_{\mathrm{ch},i}$ of every R-SET implies a different the charging time and, as a result, a different average frequency even when subject to the same potential. Figure 9(a) shows the image processing with an ensemble of identical and diverse R-SETs. The diversity of R-SETs is modelled with parameter δ, so that the charging resistance of R-SET i is given by a random value in the interval $R_{\mathrm{ch}}(1-\delta) \leq R_{\mathrm{ch},i} \leq R_{\mathrm{ch}}(1+\delta)$, with $R_{\mathrm{ch}} = 10$ GΩ. Similarly, the tunnelling

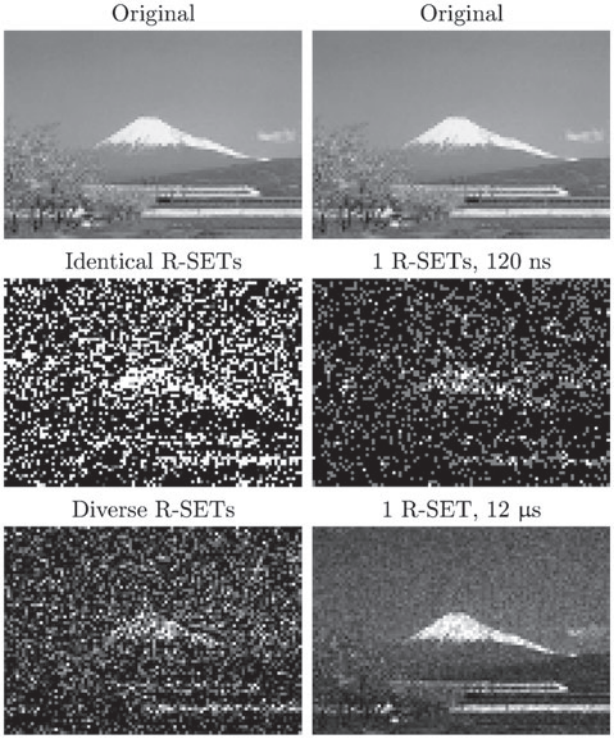

Figure 9. Two different attempted solutions for the global noise: (a) Image processing by an ensemble of identical and diverse 100 R-SETs when a a common (global) white noise has been added to the sub-threshold input potential. (b) Image processing by an single R-SETs of a sub-threshold input potential with the addition of white noise for different measuring windows times.

resistance of R-SET i takes a random value in the interval $R(1-\delta) \leq R_i \leq R(1+\delta)$, with $R = 10$ MΩ, and its capacitance is given by a random value in the interval $C(1-\delta) \leq C_i \leq C(1+\delta)$, with $C = 1$ aF. Note that for $\delta = 0$ we have the ensemble of identical R-SETs used so far (it is labelled 'identical' in Figure 9(a)). For the ensemble with diverse R-SETs, we have used $\delta = 0.25$. The introduction of heterogeneity in the ensemble gives only a slight improvement on the processed image as compared to the ensemble of identical R-SETs (Figure 9(a)). This is probably due to the fact that the 'dynamic noise' of the input potential is larger than the 'static noise' given by the diversity of the R-SETs.

We have, however, another possible way to cancel out the fluctuations by averaging over time [13]. Figure 9(b) shows the processing of the image using a single R-SET for very long measuring times. Because we employ white noise, the long time window allows for partially cancelling out the fluctuations so that the processing becomes possible. We must observe, however, that the aim of the signal transmission is basically to deliver the highest amount of information in the shortest time. In this context, a large increase of time cannot be an appropriate solution.

5. Conclusions

We have studied how noise can assist image processing in an R-SET model. Every pixel of the image is codified in an input potential that is proportional to its grey level. Because this codified potential is always sub-threshold, we have studied if a background white noise of high amplitude is able to allow an ensemble of R-SETs processing the image, similarly to what has been observed for the visual detection in humans. The results are compared with a different solution where a constant offset potential is used to scale up the codified potential to supra-threshold values. Both solutions allow the ensemble to process the image, although neither does it perfectly. The offset potential reduces the number of

grey levels of the original images whereas when noise is used, the fluctuations cannot be completely cancelled out even when a redundant system (an ensemble of R-SETs) is used. However, in the latter case the processing can be improved by increasing the number of elements in the ensemble. This is possible because the applied noise is white and local to every R-SET in the ensemble. However, when a global noise is applied to the whole ensemble, image processing is no longer possible as all R-SETs follow exactly the same pattern. A small improvement is obtained using an ensemble of diverse R-SETs because they react differently to the input signal. This result is attributed to having a much higher dynamic noise (input white noise) than static noise (diversity). In this case, the image processing can be improved by increasing the measuring time, so that we can average out the fluctuations.

Disclosure statement

No potential conflict of interest was reported by the authors.

Funding

This work was supported by the Ministerio de Economía y Competitividad [project number MAT2015-65011-P] and the Generalitat Valenciana [project number Prometeo/GV/0069].

ORCID

J. Cervera http://orcid.org/0000-0001-8965-9298
J. A. Manzanares http://orcid.org/0000-0002-5402-6842
S. Mafe http://orcid.org/0000-0003-3248-7020

References

[1] Keyes RW. Fundamental limits of silicon technology. Proc IEEE. 2001;89:227–239.
[2] Calhoun BH, Cao Y, Li X, et al. Digital circuit design challenges and opportunities in the era of nanoscale CMOS. Proc IEEE. 2008;96:343–365.
[3] Likharev KK. Single-electron devices and their applications. Proc IEEE. 1999;87:606–632.
[4] Korotkov AN. Intrinsic noise of the single-electron transistor. Phys Rev B. 1994;49:10381–10392.
[5] Kish LB. End of Moore's law: thermal (noise) death of integration in micro and nano electronics. Phys Lett A. 2002;305:144–149.
[6] Haensch W, Nowak EJ, Dennard RH, et al. Silicon CMOS devices beyond scaling. IBM J Res Dev. 2006;50:339–361.
[7] Stein RB, Gossen ER, Jones KE. Neuronal variability: noise or part of the signal? Nat Rev Neurosci. 2005;6:389–397.
[8] White JA, Rubinstein JT, Kay AR. Channel noise in neurons. Trends Neurosci. 2000;23:131–137.
[9] Rubinstein JT. Threshold fluctuations in an *N* sodium channel model of the node of Ranvier. Biophys J. 1995;68:779–785.
[10] Barber MJ, Ristig ML. Multiple thresholds in a model system of noisy ion channels. Phys Rev E. 2006;74. Article ID: 041913.
[11] Chen HS, Zhang JQ, Liu JQ. Structural-diversity-enhanced cellular ability to detect subthreshold extracellular signals. Phys Rev E. 2007;75. Article ID: 041910.
[12] Lesne A. Robustness: confronting lessons from physics and biology. Biol Rev. 2008;83:509–532.
[13] Faisal AA, Selen LPJ, Wolpert DM. Noise in the nervous system. Nat Rev Neurosci. 2008;9:292–303.
[14] McDonnell MD, Ward LM. The benefits of noise in neural systems: bridging theory and experiment. Nat Rev Neurosci. 2011;12:415–425.
[15] Ermentrout GB, Galán RF, Urban NN. Reliability, synchrony and noise. Trends Neurosci. 2008;31:428–434.
[16] Moss F, Ward LM, Sannita WG. Stochastic resonance and sensory information processing: a tutorial and review of application. Clin Neurophysiol. 2004;115:267–281.
[17] Deco G, Rolls ET, Romo R. Stochastic dynamics as a principle of brain function. Prog Neurobiol. 2009;88:1–16.
[18] McDonnell MD, Abbott D. What is stochastic resonance? definitions, misconceptions, debates, and its relevance to biology. PLoS Comput Biol. 2009;5. Article ID: e1000348.
[19] Gammaitoni L, Hänggi P, Jung P, et al. Stochastic resonance. Rev Mod Phys. 1998;70:223–287.
[20] Hirano Y, Segawa Y, Kawai T, et al. Stochastic resonance in a molecular redox circuit. J Phys Chem C. 2012;117:140–145.

[21] Oya T, Asai T, Kagaya R, et al. Stochastic resonance among single-electron neurons on Schottky wrap-gate devices. In: Ishii K, Natsume K, Hanazawa A, editors. The 2nd international conference on brain-inspired information technology held between 7 and 9 October 2005. Hibikino, Kitakyushu, Japan: Elsevier; 2006. p. 213–216.
[22] Oya T, Asai T, Kagaya R, et al. Neuronal synchrony detection on single-electron neural networks. Chaos Solitons Fract. 2006;27(4):887–894.
[23] Oya T, Asai T, Amemiya Y. Stochastic resonance in an ensemble of single-electron neuromorphic devices and its application to competitive neural networks. Chaos Soliton Fract. 2007;32:855–861.
[24] Cervera J, Manzanares JA, Mafe S. Bio-inspired signal transduction with heterogeneous networks of nanoscillators. Appl Phys Lett. 2012;100. Article ID: 093703.
[25] Cervera J, Manzanares JA, Mafe S. Biologically inspired information processing and synchronization in ensembles of non-identical threshold-potential nanostructures. PLoS One. 2013;8. Article ID: e53821.
[26] Simonotto E, Riani M, Seife C, et al. Visual perception of stochastic resonance. Phys Rev Lett. 1997;78:1186–1189.
[27] Kano S, Tadaa T, Majima Y. Nanoparticle characterization based on STM and STS. Chem Soc Rev. 2015;44:970–987.
[28] Kasai S, Asai T. Stochastic resonance in Schottky wrap gate-controlled GaAs nanowire field effect transistors and their networks. Appl Phys Express. 2008;1. Article ID: 083001.
[29] Kasai S, Miura K, Shiratori Y. Threshold-variation-enhanced adaptability of response in a nanowire field-effect transistor network. Appl Phys Lett. 2010;96. Article ID: 194102.

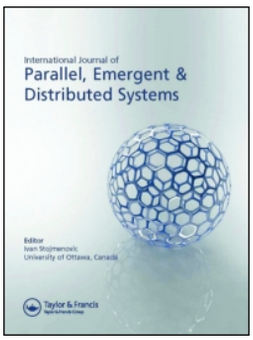

International Journal of Parallel, Emergent and Distributed Systems

ISSN: 1744-5760 (Print) 1744-5779 (Online) Journal homepage: http://www.tandfonline.com/loi/gpaa20

Noise assisted image processing by ensembles of R-SETs

J. Cervera, J. A. Manzanares & S. Mafe

To cite this article: J. Cervera, J. A. Manzanares & S. Mafe (2017) Noise assisted image processing by ensembles of R-SETs, International Journal of Parallel, Emergent and Distributed Systems, 32:3, 295-305, DOI: 10.1080/17445760.2017.1316908

To link to this article: http://dx.doi.org/10.1080/17445760.2017.1316908

Published online: 26 Apr 2017.